Damping Adaptive Neural Controller Design in HVDC based on Offshore Wind Turbine to Improve Power System Stability

A. Hamidi[1]; J. Beiza[2,*]; T. Abedinzadeh[3]; A. Daghighi[4]

1- Department of Electrical Engineering, Shabestar Branch, Islamic Azad University, Shabestar, Iran, Email: abdolkhalegh.hamidi@iauyasooj.ac.ir
2- Department of Electrical Engineering, Shabestar Branch, Islamic Azad University, Shabestar, Iran, Email: jamalbeiza@gmail.com
*corresponding author
3- Department of Electrical Engineering, Shabestar Branch, Islamic Azad University, Shabestar, Iran, Email: taherabedinzade@yahoo.com
4- Department of Electrical Engineering, Shabestar Branch, Islamic Azad University, Shabestar, Iran, Email: A_daghigh@sbu.ac.ir

Received: 2020-06-25
Revised: 2021-01-09
Accepted: 2021-04-22

Abstract Because of low losses and voltage drop, fast control of power, the limitless connection distance and isolation issues, using the High Voltage Direct Current (HVDC) transmission system based on Voltage Source Converters (VSC) is recommended to the power transfer in the electrical power networks included the offshore wind power plants (OWPP). The OWPPs are expected to meet the grid code necessities when requested to maintain stability. Utilization of the VSC HVDC along with the OWPP, can improve the control of power flow and the power system dynamic stability. In this paper, the impact of control of VSC HVDC based OWPP, on the dynamic stability of power systems is evaluated. In this way, the dynamic modeling of power system equipped by the VSC HVDC and OWPP are proposed. In the proposed model, using the concepts of controllability and observability of electromechanical modes of power systems, a new approach to the design a supplementary damping controller in VSC HVDC based OWPP is presented. The damping controller is designed based on the nonlinear adaptive neural networks concepts and trained by a proposed online method. The simulation results which are done in MATLAB, show the effectiveness of the proposed control strategy.

Keywords: Offshore wind turbine, VSC HVDC systems, damping adaptive neural controller, control configuration analysis.

1. Introduction

Todays, using of clean and renewable energy are considered by a lot of power systems experts due to the negative effects of fossil fuels such as environmental pollution, global warming and climate change[1]. Different kind of renewable energy sources such as Photovoltaic Cells, Geothermal, wind turbines, etc are used in power systems to generate electricity. Among those, wind energy is one of the fastest growing renewable energy resources which has noticeable potential to generate electrical power[2-3]. The researchers believe that wind turbines can provide more than 20 percent of the world's energy needs. The high electrical power can be generated from an aggregation of multiple wind turbines as a wind farm or wind park. With the increasing penetration of wind turbines in power grids, using appropriate interconnections and control structures will be essential to ensure power system stability, power quality and reliability[3-5]. Todays, because of the enormous wind resources in the seas, using wind turbines installed at far distance of shore has been increased. This technology which is known as offshore wind turbine has been developed since 2000s. wind speed over the ocean are much higher and much more consistent rather than onshore wind, so wind turbines optimized for the most common wind speed over the ocean will operate at very high efficiencies relative to similarly optimized turbines onshore[5]. Furthermore, wind speeds offshore are increased in the afternoon which is the time for increasing power demand (as opposed to onshore wind speeds which tend to increase overnight). Also, wind farms views are not attractive and moving them onto seas can solve this problem [5-6]. However, by increasing the capacity and distance of wind farms from shore, the methods for connection wind power plants to the main network in shore became important. Optimal utilization of offshore wind turbines requires the use of appropriate, reliable and efficient transmission systems[7-8]. Offshore wind farms produce AC power and using high voltage alternative current (HVAC) transmission system can be easiest solution. HVACs are well known technology, installed easily and affordable in terms of cost. Nevertheless, reactive power and insulation

restrictions become a limit of this kind of transmission systems[9-10].

HVDC systems connect developed power systems and offer economic and technical benefits. The application of the HVDC transmission lines include for example non-synchronous interconnection, control of power flow, and modulation to increase stability limits. The transient stability of the AC systems in a composite AC–DC system can be improved by taking advantage of the fast controllability of HVDC converters. Therefore, it is better to combine HVDC transmission systems close to HVAC lines. The VSC HVDC system is the modern HVDC technology. It consists of two VSCs, one of them operates as a rectifier and the other one acts as an inverter. The two converters are connected through a DC line. Its main function is to transmit a constant DC power from the rectifier station to the inverter station, with high controllability. In recent years, using of High Voltage Direct Current (HVDC) transmission systems has proposed for offshore wind turbines as a solution for mentioned problem. HVDC systems not only obtain appropriate path to transfer power but also participate in stabilizing main power systems[10-11].

In [11] pointed out that oscillation modes of power system can be controlled through a supplementary controller which is designed for HVDC. In [12] an adaptive damping controller is designed in VSC HVDC system to damp low frequency oscillations in power system. Authors in [12] show that, it is possible to apply damping signal to each control signal of converters in VSC HVDC system but impacts of each input signal on the electromechanical modes are different.

The oscillation modes, in a power system with high penetration of wind turbines, have weak controllability and observability. Therefore, their diagnosis will be complicated and control strategies definition to prevent system instability would be problematic. It should be noted that wind turbines farms have fundamentally different structure rather than classical power plants and so, cannot support voltage and frequency of network, especially under fault conditions.

In [13], it is mentioned that electromechanical oscillations of a wind turbine are excited during the high wind speed. This can lead to the destruction of the dynamic stability of the whole power system. The purpose of the paper is to find out the nature and reason of the above-mentioned electromechanical oscillations based on speed-power curve of a wind turbine. It is shown that at some operating points, low frequency oscillations with frequency of 2 Hz appear on the generator power, generator speed and shaft torsional torque. For improving the damping of the torsional modes, an auxiliary stabilizer control, known as torsional oscillations stabilizer (TOS), is proposed. The proposed controller not only improve the dynamic stability of mechanical part of wind turbine but also lead to improvement of power system dynamic stability.

In [14], it is pointed that integration of large-scale wind farms into power systems presents some challenges such as dynamic stability must be addressed and analysed. This paper presents a systematic approach to design a classical lead-lag power system stabilizer (PSS) for improving the stability of the system following a small disturbance. it is shown that the dynamic stability of the system will be improved considerably when the PSS is installed in wind farm. In mentioned paper, it is not clear how wind turbines affect oscillating modes.

In [15], the effect of wind turbines with VSC HVDC transmission systems on the oscillation modes of the network is evaluated. In this study, it is shown that the electromechanically modes of the power system are affected by the power flow in HVDC lines and so controlling this power can affect the stable performance of the modes.

Generally, the growing penetration of offshore wind turbines installed without taking the requirements and standards into account, can undermine the stability and reliability of the power system. Offshore wind turbines equipped by VSC HVDC systems will be an appropriate opportunity not only for transmission of power generated but also to improve power system stability. In such a multi-input, multi output (MIMO) systems, recognition of best input-output signal coupling, which has most effective on oscillation modes, will be important. In this case, it will be possible to design supplementary controller to enhance power system performance. So far, the influence of wind turbines on power system stability, appropriate input-output signal selection and damping controller design have been studied in many literatures[7-11]. However, such study has not been achieved for offshore wind turbine equipped by VSC HVDC systems. In this paper, modelling of a power system including wind turbines, VSC HVDC transmission system and synchronous generator will be discussed. Using of obtained model, oscillating mode is recognized. controllability and observability of oscillation mode will be measured through singular value decomposition (SVD) concept. This can help us to select most appropriate input-output signal to design damping supplementary controller. In this study, supplementary controller is designed based on neural network concepts. Proposed neural controller is an adaptive controller which can damp oscillations in different working condition.

2. Power system modelling

Power system under study is shown in Fig.1. this system includes wind turbine, VSC HVDC transmission system, synchronous generator and infinite bus. DC link capacitance is used to regulate output voltage of converters. Inductance are used to model inductive property of transmission and coupling transformers. Power losses are not considered. $M_{1,2}$ and $\delta_{1,2}$ show modulation index and phase angle of each converter, respectively. Terminal voltage of wind turbine is shown by $V_w \angle \theta_w$.

Wind turbine based on DFIG has dynamic which is faster than electromechanical (EM) modes. In this turbine, it is possible to control generated active power through generator side converter while exchanged reactive power is controlled through grid side converter. On the other hand, using converters of DFIG it is possible to decouple wind turbine from network. So, wind turbines act as a negative load which exchange active and reactive power with utility and is controlled by local controller. Voltage of wind turbine (negative load) terminal is important from network perspective and must regulate in an

appropriate value. In this paper this component is considered as an output of system.

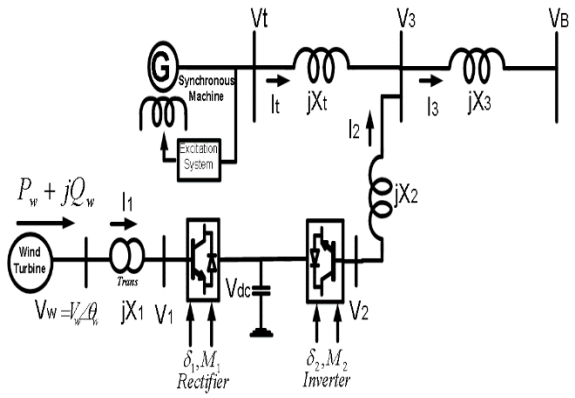

Fig. 1. Power System equipped by Offshore Wind Turbine and VSC HVDC System

In this study, the wind turbine is considered as a negative load [6]. By circuit analyzing of Fig.1 an daccording what is mentioned in Appendix, synchronous generator injected current can be obtained:

$$I_{tq} = Z_6 . M_2 . V_{dc} . cos\ \delta_2 - Z_7\ sin\ \delta \tag{1}$$

By linearization (1):

$$\Delta I_{tq} = Z_{11}\Delta M_2 + Z_{12}\Delta V_{dc} + Z_{13}\Delta\delta_2 + Z_{14}\Delta\delta \tag{2}$$

Based on Park transformation, power balance relationship for HVDC can be written:

$$\frac{dV_{dc}}{dt} = \frac{3M_2}{4C_{Dc}}\left(cos\ \delta_2\, I_{2d} + sin\ \delta_2 I_{2q}\right) \tag{3}$$

The above equation mentioned that injected power from AC system side to DC line is equal with saved energy in capacitance. To obtain state space model of whole power system, iot is essential to linearize (3) . in this way I_{2d} ، I_{2q} ، I_{1d} and I_{1q} are calculated based on states variables and linearized around the working point:

$$\begin{aligned}
&\Delta I_{2d} = Z_{25}\Delta E'_q + Z_{26}\Delta M_2 + Z_{27}\Delta V_{dc} \\
&+Z_{28}\Delta\delta_2 + Z_{29}\Delta\delta \\
&\Delta I_{2q} = Z_{35}\Delta M_2 + Z_{36}\Delta V_{dc} + Z_{37}\Delta\delta_2 \\
&+Z_{38}\Delta\delta \\
&\Delta I_{1d} = Z_{39}\Delta P_\omega + Z_{40}\Delta\theta_\omega + Z_{43}\Delta M_1 \\
&+Z_{44}\Delta\delta_1 + Z_{25}\Delta V_{dc} \\
&\Delta I_{1q} = Z_{46}\Delta\theta_\omega + Z_{47}\Delta P_\omega + Z_{48}\Delta\delta_1
\end{aligned} \tag{4}$$

Substituting (4) in (3), we will have:

$$\begin{aligned}
\Delta\dot{V_{dc}} = {} & Z_{56}\Delta M_2 + Z_{57}\Delta M_1 + Z_{58}\Delta\delta_1 \\
&+Z_{59}\Delta\delta_2 \\
&+Z_{60}\Delta V_{dc} + Z_{61}\Delta E'_q + Z_{62}\Delta\delta + Z_{63}\Delta P_\omega
\end{aligned} \tag{5}$$

Similarly for injected active power into the power grid by synchronous and also $P_e = V_d I_d + V_q I_q$ we can write:

$$\Delta P_e = a_4\Delta M_2 + a_5\Delta\delta_2 + a_6\Delta\delta + a_7\Delta V_{dc} \tag{6}$$

On the other hand, teminal voltage of wind turbine must be linearized:

$$\Delta V_t = a_{12}\Delta M_2 + a_{13}\Delta V_{dc} + a_{14}\Delta E'_q + a_{15}\Delta\delta_2 \tag{7}$$

Nonlinear model of synchronous generator is written as follow:

$$\begin{aligned}
&\dot{\delta} = \omega_0\omega \\
&\dot{\omega} = \frac{P_m - P_e - D\omega}{2H} \\
&\dot{E'_q} = \frac{-E_q + E_{fd}}{T'_{do}}
\end{aligned} \tag{8}$$

In above equation, δ , P_m, P_e, ω, E'_q, E_{fd}, T'_{do}, V_t, V_{t0}, K_A , T_A are load angle, mechanical power applied by turbine, injected electrical power, rotor speed deviation, voltage behind of synchronous reactance , excitation voltage, transiant time constant, voltage ampitude of terminal, refrence voltage , gain and time constant of excitation respectively. Also we have following equations which explaine relations between mentioned variables:

$$\begin{aligned}
T_e = P_e = V_{td}I_{td} + V_{tq}I_{tq}, V_{td} &= x_q i_{tq}, V_{tq} \\
&= E'_q - x'_d i_{td} \\
E_q &= E'_q + (x_d - x'_d) i_{td}
\end{aligned} \tag{9}$$

Using above equation, following model (10) is obtained as state space model of power system.

Block diagram of (10) is shown in Fig.2. $K_{pu}, K_{qu}, K_{vu}, K_{cu}$ are vectors which show corresponding row of each state variable in B matrix in state space model. State variables are introduced as: $\Delta\delta$ (load angle), $\Delta\omega$ (rotor speed deviation), $\Delta E'_q$ (voltage behind synchronou reactance), ΔE_{fd} (excitation voltage) abd ΔV_{dc} (voltage of DC line). Input variables are $\Delta\delta_i$ (modulation angle), ΔM_i (modulation index), ΔP_w (Active power deviation in wind turbine), ΔQ_w (Reactive power deviation in wind turbine), ΔU_{pss} (deviation of power system stablizer signal).

$$\begin{bmatrix} \Delta\dot{\delta} \\ \Delta\dot{\omega} \\ \Delta\dot{E}'_q \\ \Delta\dot{E}_{fd} \\ \Delta\dot{V}_{dc} \end{bmatrix} = \begin{bmatrix} 0 & \omega_0 & 0 & 0 & 0 \\ -\frac{a_6}{M} & -\frac{D}{M} & -\frac{a_8}{M} & 0 & -\frac{a_7}{M} \\ \frac{sZ_{18}}{T'_{do}} & 0 & \frac{sZ_{10}}{T'_{do}} & \frac{1}{T'_{do}} & \frac{sZ_{16}}{T'_{do}} \\ -\frac{K_A a_{16}}{T_A} & 0 & -\frac{K_A a_{14}}{T_A} & -\frac{1}{T_A} & -\frac{K_A a_{13}}{T_A} \\ t\_Z_{62} & 0 & t\_Z_{61} & 0 & t\_Z_{60} \end{bmatrix} \begin{bmatrix} \Delta\delta \\ \Delta\omega \\ \Delta E'_q \\ \Delta E_{fd} \\ \Delta V_{dc} \end{bmatrix} + \begin{bmatrix} 0 & 0 & 0 & 0 & 0 & 0 & 0 \\ 0 & 0 & -\frac{a_4}{M} & -\frac{a_5}{M} & 0 & 0 & 0 \\ 0 & 0 & \frac{sZ_{15}}{T'_{do}} & \frac{sZ_{17}}{T'_{do}} & 0 & 0 & 0 \\ 0 & 0 & -\frac{K_A a_{12}}{T_A} & -\frac{K_A a_{15}}{T_A} & 0 & 0 & \frac{K_A}{T_A} \\ t\_Z_{57} & t\_Z_{58} & t\_Z_{56} & t\_Z_{59} & t\_Z_{63} & t\_Z_{64} & 0 \end{bmatrix} \begin{bmatrix} \Delta M_1 \\ \Delta\delta_1 \\ \Delta M_2 \\ \Delta\delta_2 \\ \Delta P_w \\ \Delta Q_w \\ \Delta U_{pss} \end{bmatrix} \quad (10)$$

3. Input-Output signal selection based on SVD

In this study, input-output signal selection will be done based on concepts of controllability and observability and their relations to singular value decomposition of a matrix. Controllability is an important property of a control system, and the controllability property plays a crucial role in many control problems, such as stabilization of unstable systems by feedback, or optimal control. Controllability and observability are dual aspects of the same problem. Observability is a measure for how well internal states of a system can be inferred by knowledge of its external outputs [15-16]. A system in state space form $\dot{x} = Ax + Bu$ is controllable if for any initial state $x(t_0), t_1 > 0$ and final state x_1 , there is a limited input as $x(t_1) = x_1$. This system is called observable if for any $t_1 > 0$, the value of initial state be detemined using $u(t_1)$ and $y(t_1)$ [17]. PBH test is used to detemine observability and controllaility in a dynamic system. PBH test is used to assess the following matrices rank:

$$C(\lambda_k) = [\lambda_k I - A, b_i] \quad (11)$$

Where, λ_k is a Kth eigen value of matrix A. I is a unit matrix, b_i is corresponding column of ith input in B matrix and c_j is a corresponding row of jth output.

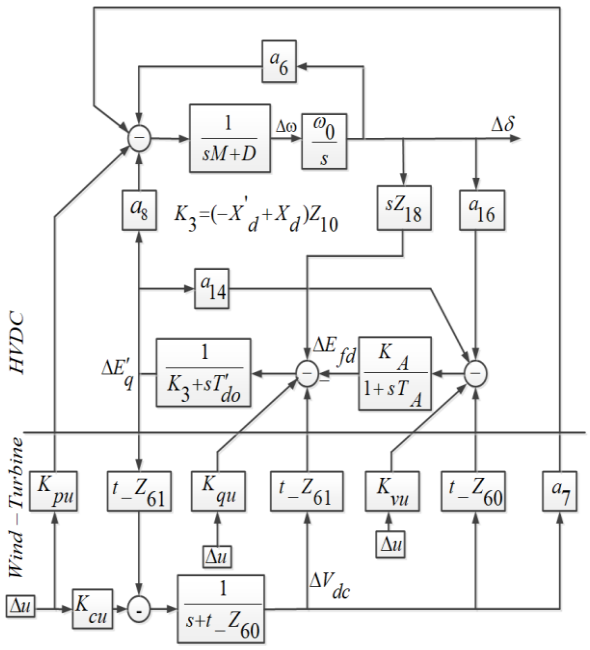

Fig. 2. block diagram of (10)

λ_k in a linear system is controllable if $C(\lambda_k)$ matrix be full rank. Similarly, λ_k is observable if $O(\lambda_k)$ be full rank. Rank of a matrix can be calculated using minimum singular value. λ_k is controllable (observable) if matrix $C(\lambda_k)$ ($O(\lambda_k)$)be a full rank matrix. Singular value decomposition of a matrix can be used to calculate rank value. Input-output signal selection based on PBH test is explained by an algorithm which is shown in Fig.11. selecting most appropriate input-output coupling, designing a supplementary controller will be critical in next step.

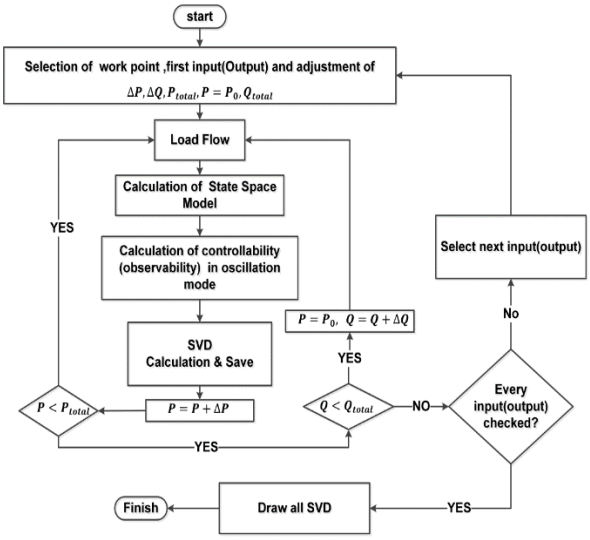

Fig. 3. proposed algorithm to obtain most appropriate input-output coupling

4. Adaptive damping neural controller design

As mentioned in previous section, Power system has nonlinear characteristic and any change in environmental parameters can effect on output voltages and currents. So, it is desirable that identifies power system characteristic in any time step to implement most effective supplementary damping controller. In this part of paper, using an adaptive nonlinear neural controller is proposed.

The simplest definition of neural networks is as follows:"a computing system made up of a number of simple, highly interconnected processing elements, which process information by their dynamic state response to external inputs". Neural networks are usually composed of several layers. In each layer, there are interconnected neurons which include activation function [18-19].

Data are applied to the input layer and after that will be communicated with one or several hidden layers. In neural networks actual processing is done via a system of

weighted 'connections'. Notice that hidden layers are connected to the output layer which produce final output of network. Modifing of weights are done using many different learning rules like delta rule. The delta rule is often utilized by the most common class of neural netwroks and works based on error backpropagation algorithm [20-21].

Fig.4. shows the proposed adaptive neural controller for damping application. This adaptive neural controller includes two separated neural networks as identifier and controller. Neural controller is used to generate damping signal and neural identifier is used to model dynamic of the power system and to adapt the neuro controller parameters. On the other hand, Neural identifier is a feed forward multilayer perceptron while neural controller is working based on recurrent neural networks. Using output components of real power system and outputs of neural controller, it will be possible to train neural identifier based on error back propagation method. Dash lines in Fig. 4 show the back propagation paths to update the weights of the neural identifier and controller.

Cost function for identifier, which must be minimized to train neural network, is defined as sum of square difference between rotor speed deviation of real power system and output of identifier in each time sample respectively as follow:

$$e_{id} = \frac{1}{2}\{(\omega - \omega')^2\} \quad (12)$$

Neural controller, which is a recurrent neural network, has important task. It is responsible to produce appropriate damping signal. In addition to the rotor speed deviations samples, past outputs of controller are fed to the network. The neural controller is trained using back propagation error method. For this network error is calculated as follow:

$$e_{co} = \frac{1}{2}\{(\omega_{ref} - \omega')^2\} \quad (13)$$

Notice that, to train neural controller, error in (13) must back propagate using neural identifier path. Also, for getting best result it is essential to have $\omega_{ref} = 0$

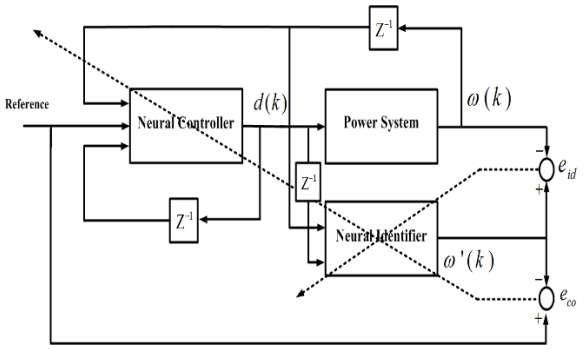

Fig. 4. Proposed Adaptive Neural Controller based on Damping Controller

4.1. Neural Identifier

The neural identifier is developed based on series parallel auto regressive moving average (NARMA) model. Every output of identifier at time k+1 depends on both past n values of output and m past values of inputs. Because of limitations in computations, the selected value for m and n should not be too large. Neural identifier will be used in proposed control structure for two purposes: (a) identification of power system and (b) training neural controller based back propagation error and delta rule. As it is shown in Fig.4 error of $\frac{dp}{dv}$ deviation must back propagate using neural identifier to update connection weights in neural controller. There is no alternative to train neural controller. Structure of neural identifier is shown in Fig.5. This network has four neurons at hidden and one at output layer. F is activation function that is hyperbolic tangent in this paper. It is trained using error back propagation method that described in detail in following.

Cost function is defined as (12). Using relative derivatives, it is possible to write:

$$\frac{\partial E_{id}}{\partial w^{id}{}_{oh}} = \frac{\partial E_{id}}{\partial e_{id}} \frac{\partial e_{id}}{\partial (\hat{\Delta\omega})} \frac{\partial (\hat{\Delta\omega})}{\partial v} \frac{\partial v}{\partial w^{id}{}_{oh}} \quad (14)$$

Where $w^{id}{}_{oh}$ are used to show connected weights between output and hidden layer. Based on (13), sensetivve coefficients ot neuron in output layer is calculated and w_{oh}^{id} will be updated. To update and corrects weights between input-output layers, sensitive coefficients of neurons in output layer must be used.

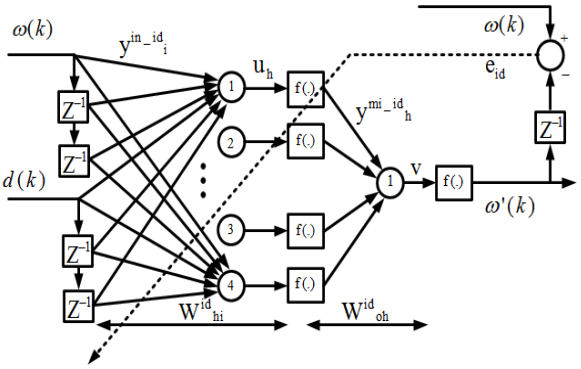

Fig. 5. Structure for Proposed Adaptive Identifier

$$w^{id}{}_{oh\,New} = w^{id}{}_{oh\,Old} - \eta \frac{\partial E_{id}}{\partial w^{id}{}_{oh}} \quad (15)$$

4.2. Neural Controller

Fig.6. shows the structure of proposed adaptive neural controller in detail. This network is a recurrent neural network. A recurrent neural network (RNN) is a class of artificial neural network where connections between units form a directed cycle. This structure

creates an internal state of the network which allows it to exhibit dynamic temporal behavior. Unlike feedforward neural networks, RNNs can use their internal memory to process arbitrary sequences of inputs.Cost function to training this network is defined based on (13). To minimize cost function, we can write:

$$\frac{\partial E_{co}}{\partial(\omega')} = e_{co} \tag{16}$$

$$\frac{\partial E_{co}}{\partial w^{co}{}_{oh}} = \frac{\partial E_{co}}{\partial e_{co}} \frac{\partial e_{co}}{\partial(\hat{\Delta\omega})} \frac{\partial(\hat{\Delta\omega})}{\partial v} \frac{\partial v}{\partial w^{co}{}_{oh}} \tag{17}$$

V, $w^{co}{}_{oh}$ are the neural identifier output and the weights between output and hidden layer of neural controller, respectively.

$$v = \sum_h w^{id}{}_{oh} y^{mi\_id}{}_h$$
$$y^{mi\_id}{}_h = f(\sum_i w^{id}{}_{hi} y^{in\_id}{}_i) = f(u_h) \tag{18}$$

$y^{in\_id}{}_i$, $y^{mi\_id}{}_h$, $w^{id}{}_{hi}$, $w^{id}{}_{oh}$, i and h are inputs , inputs to output layer, connection weights between input and hidden layer, weights between output and hidden layer, number of inputs and number of neuron in hidden layer of neural identifier, respectively. where:

$$\frac{\partial v}{\partial w^{co}{}_{oh}} = \frac{\partial v}{\partial U_c} \frac{\partial U_c}{\partial w^{co}{}_{oh}} = \frac{\partial v}{\partial y^{mi\_id}{}_h} \frac{\partial y^{mi\_id}{}_h}{\partial U_c} \frac{\partial U_c}{\partial w^{co}{}_{oh}} \tag{19}$$

Using (17-19), it is possible to calculate the sensitive coefficient in output neuron of neural controller and correct the middle and output weights of neural controller.

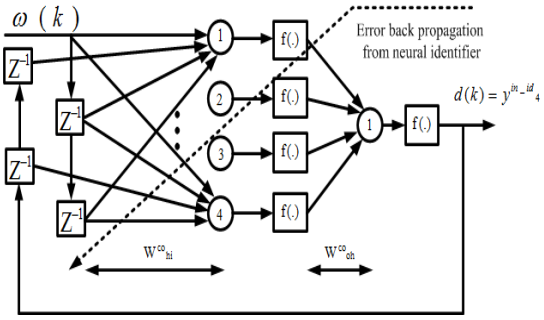

Fig. 6. Structure of the online neural controller

4.3. Training Process

Training process will be done in

4.3.1 Pre-Control Phase

Before implementation of proposed neural controller for power system, neural identifier will trainee offline. To reach this goal, power system without damping controller will simulated and data of this system will be saved. Then, data are used to train neural identifier in offline mode. After this step, a random input will be giving to power system and neural identifier simultaneously and system runs. The procedure which was explained in section 1 will be used to train network (Fig.7). in cascade with neural identifier, neural controller is trained. Connection weights of neural controller must be corrected using neural identifier path which is shown in Fig.8. by dash line.

4.3.2 Post Control Phase

In this phase of training, both identifier and controller neural networks are used simultaneously.

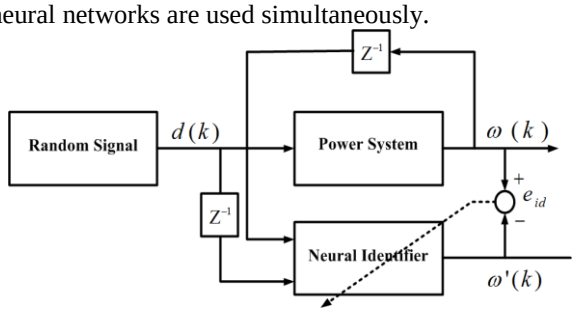

Fig. 7. training of neural identifier in pre control phase

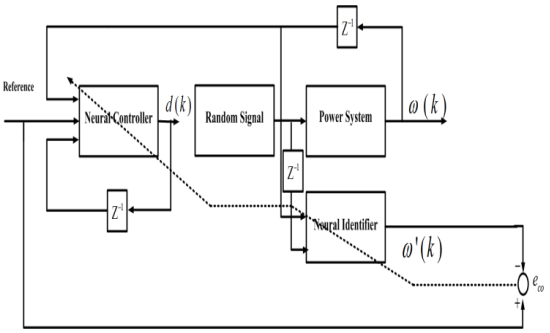

Fig. 8. training of neural controller in pre control phase

During this process, neural identifier training is achieved through the back-propagation error between real power system and neural identifier outputs. After updating of connected weights in neural identifier, training of neural controller will be done using identifier path. Finally, neural controller output is calculated and applied to the power system.

5. Simulation results

Proposed algorithm (Fig.3) is used to measure controllability and observability of oscillation mode in modelled power system. MATLAB software is used to do all simulation. A supplementary controller is designed based on adaptive neural network which has been explained in previous section. Parameters of power system and neural controller are given in appendix. Working condition of wind turbine is selected as table.1 to determine its effects on controllability (observability) of oscillation mode.

Table 1. Working condition of wind turbine as a negative load.

Power	P_w	Q_w
Light (μ_1)	0.9pu	0.1pu
Heavy (μ_2)	1.2pu	0.4pu

Fig.9 and Fig.10 show results of controllability and observability of oscillation mode . in Fig.9 it is observed that, controllability of oscillation mode is more , through the input of modulation index in inverter, rather than other inputs. So this input can be a appropriate to apply damping signal.

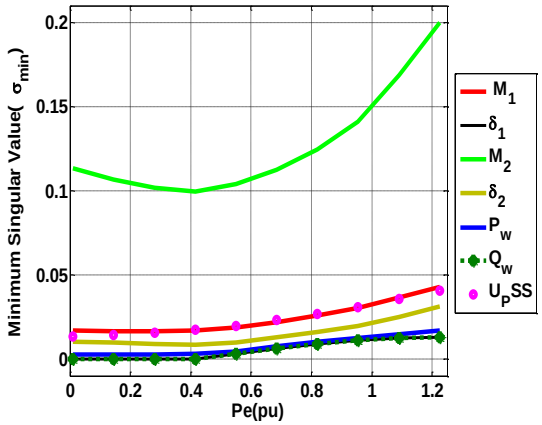

(a)

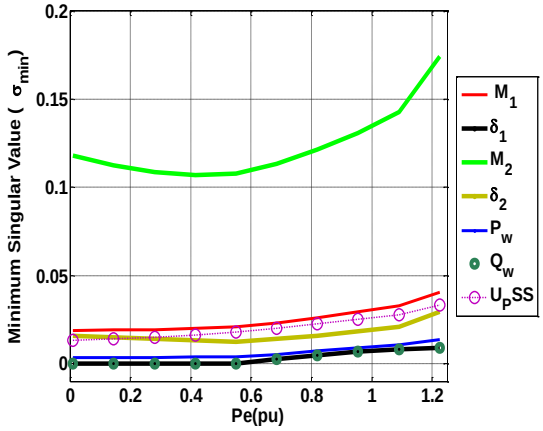

(b)

Fig. 9. Controllability of oscillation mode through the inputs. (a) Light condition (μ_1), (b) Heavy condition (μ_2).

Between other inputs, modulation index of rectifier and PSS have more controllability on oscillation mode. It must be noticed that inputs of wind turbine has weak controlability . In addition, all inputs for wind turbine have a relatively poor controllability, especially in nominal work condition of synchronous generator. Based on Fig.10, most observability of oscillation mode is measured through load angle output while least observability is achived through rotor load angle deviation. So, it can be concluded that best coupling between input-output signals based SVD results is $\delta - M_2$. After choosing best path between input-output signal, adaptive neural controller is designed to improve power system stability. For comparison purposes, besides $\delta - M_2$ path , $V_w - M_2$ also is selected to design supplementary damping controller. Ability of proposed neural controller to damp power system oscillations are shown by comparision its responses with a lead-lag controller. Neural controllers are designed based on linearized model of power system and used in nonlinear model to enhance power system performance. Active power deviation in the wind turbine with value $\Delta P_w = 0.1pu$ and time $t = 5s$ and deviation in the modulation index with value $\Delta M_1 = 0.01pu$ and time $t = 0s$ are used as a disturbances for linear system.

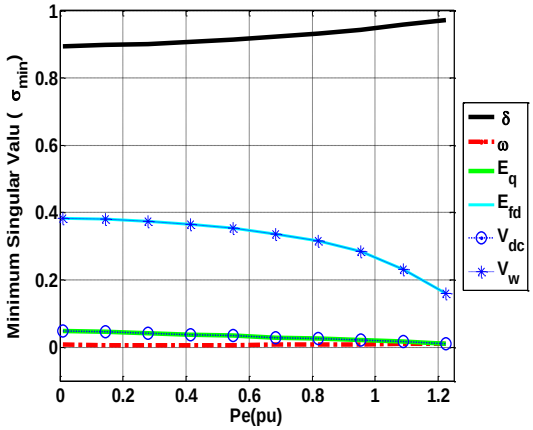

(a)

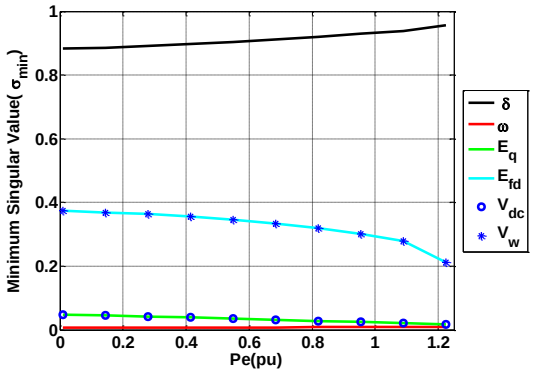

(b)

Fig. 10. observability of oscillation mode through the inputs. (a) Light condition (μ_1), (b) Heavy condition (μ_2).

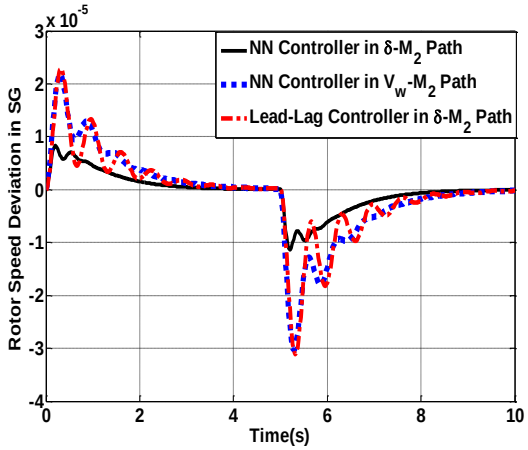

Fig. 11. rotor speed deviation (linear system)

Fig.11 shows the deviation of some neural network weights (identifier network) .

Fig.11 shows the rotor speed deviation. It is observed that nonlinear system is stablized. In addition, neural controler used in the $\delta - M_2$ shows the best response (low overshoot and settling time). Notice that controller in $V_w - M_2$ path has improved the stability of power system but its response is not better than $\delta - M_2$ path based controller. Fig.12 shows the injected active power to the main network by synchronous generator. It is observed that oscillation of power have been damped by using proposed controllers.

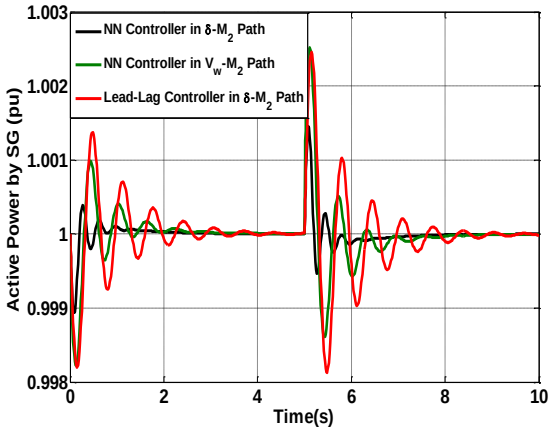

Fig. 12. injected active power deviation. by synchronous generator (linear system)

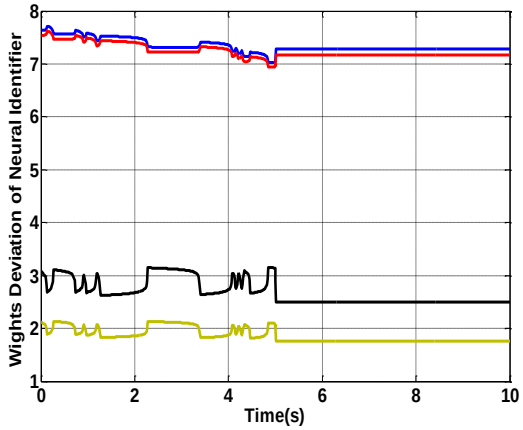

Fig. 13. deviation of neural network weights

Responses of nonlinear system simulation (for heavy load condition) equipped by neural damping controller are shown in Fig.14-16. It must be mentioned that deviation of mechanical input power at t=0 in SG $\Delta P_m = 0.05pu$ and three phase short circuit on inifity bus at t=10s for 7 cycles are considered as disturnaces.it is observed that damping neural controller can obtain best response rather than classic lead lag controller in the appropriate IO path.

6. CONCLUSION

In this paper a power system equipped by offshore wind turbine is moseled to obtain state space model. Using controllability and observability concept and their relation with SVD , input-output signal selection is achieved.

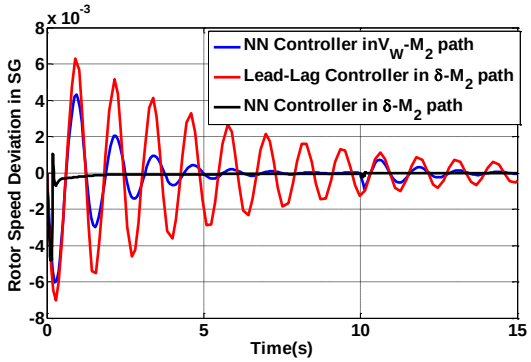

Fig. 14. rotor speed deviation (nonlinear system)

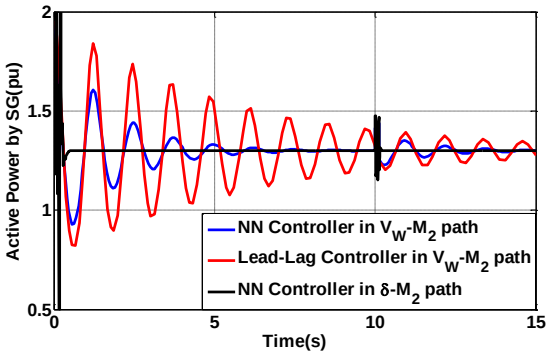

Fig. 15. injected active power deviation. by synchronous generator (nonlinear system)

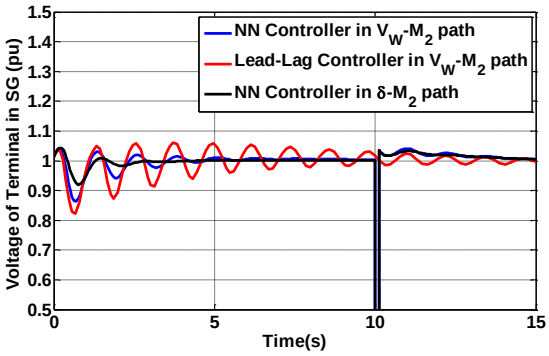

Fig. 16. voltage deviation (nonlinear system)

It is observed that each inputs of HVDC system can effect on oscillation mode but most effec can obtain using modulation index of inverter. Based on proposed input-output signal selection algorithm $\delta - M_2$ is a best path betwenn inputs-outputs which can damp power system oscillations. Proposed neural controller can stablize system better than classic lead-lad compensator.

7. References

[1] P.C. Carlos, D. Greaves, G. Iglesias, "A review of combined wave and offshore wind energy", *Renewable and Sustainable Energy Reviews*, vol. 42, no. 9, pp. 141-153, 2015.

[2] M. Shafiee, "Maintenance logistics organization for offshore wind energy: current progress and future perspectives", *Renewable Energy*, vol. 77, pp. 182-193, 2015.

[3] S. Cavazzi, A.G. Dutton, "An Offshore Wind Energy Geographic Information System (OWE-GIS) for

assessment of the UK's offshore wind energy potential", *Renewable Energy*, vol. 87, pp. 212-228, 2016.
[4] E. Mohamed, Kwok L. Lo, and O. Anaya-Lara, "Impacts of high penetration of DFIG wind turbines on rotor angle stability of power systems", *Transactions on Sustainable Energy*, vol. 63, pp. 759-76,2015.
[5] H. Ertong, and C. Liu, "Impacts of high penetration of DFIG wind turbines on rotor angle stability of power systems", *Ocean Engineering*, vol. 130, pp. 218-227,2017.
[6] D.García, José Luis, Carlos E. Ugalde-Loo, Fernando Bianchi, and Oriol Gomis-Bellmunt, "Input–output signal selection for damping of power system oscillations using wind power plants", *International Journal of Electrical Power & Energy Systems*, vol. 58, pp. 75-84,2014.
[7] J-F. Adri, Y. Pipelzadeh, and Tim C. Green, "Blending HVDC-link energy storage and offshore wind turbine inertia for fast frequency response", *Transactions on Sustainable Energy*, vol. 63, pp. 1059-1066,2015.
[8] C. Miguel Jiménez, et al, "Optimal power flow in multi-terminal HVDC grids with offshore wind farms and storage devices", *International Journal of Electrical Power & Energy Systems*, vol. 65, pp. 291-298,2015.
[9] L. Hongzhi, and Z. Chen, "Contribution of VSC-HVDC to frequency regulation of power systems with offshore wind generation", *Transactions on Energy Conversion*, vol. 30.3, pp. 918-926,2015.
[10] N. Sotirios, I. Georgios N. Patsakis, and Stavros A. Papathanassiou, "Assessment of communication-independent grid code compatibility solutions for VSC–HVDC connected offshore wind farms", *Electric Power Systems Research*, vol. 121, pp. 38-51,2015.
[11] N.Taheri, and M. Banaei, "A supplementary neural controller for novel modeling of VSC HVDC to enhance dynamic stability in a power system", *In 2010 1st Power Electronic & Drive Systems & Technologies Conference* (PEDSTC), pp. 7-12,2010.
[12] M_ R_, Banaei and N. Taheri, "An adaptive neural damping controller for HVDC transmission systems", *European Transactions on Electrical Power*, vol. 21, pp. 910-923,2011.
[13] M.Rahimi, M.R.Esmaeili, "Power controller design and damping improvement of torsional oscillations in the 710 kW DFIG based wind turbine installed at the Binalood site", *Tabriz Journal of Electrical Engineering*, vol. 46, no. 4, pp. 123-134, 2016 (in persian).
[14] R. Sayyad, A. Khodabakhshian, R. Hooshmand, "A New Systematic Design of Power System Stabilizer Using Classical and Genetic Algorithm Techniques for Wind Power Systems", *Tabriz Journal of Electrical Engineering*, vol. 39, no. 1, pp. 13-23, 2009 (in persian).
[15] N.Shafaghatian, A.Kiani, N. Taheri, Z. Rahimkhani, and S- S. Masoumi, "Damping controller design based on FO-PID-EMA in VSC HVDC system to improve stability of hybrid power system", *Journal of central south university*, vol. 2, pp. 403-417,2020.
[16] Y.ao, W.ei, et al, "Wide-area damping controller for power system interarea oscillations: a networked predictive control approach", *Transactions on Control Systems Technology*, vol. 23.1, pp. 27-36,2015.
[17] P. Manuel, G. Robledo, "Controllability and observability for a linear time varying system with piecewise constant delay", *Acta Applicandae Mathematicae*, vol. 136.1, pp. 193-216,2015.
[18] L.iu, Yan-Jun, et al, "Neural controller design-based adaptive control for nonlinear MIMO systems with unknown hysteresis inputs", *transactions on cybernetics*, vol. 46.1, pp. 9-19,2016.
[19] M. Arefi, M-R.Jahed-Motlagh, H- R. Karimi, "Adaptive neural stabilizing controller for a class of mismatched uncertain nonlinear systems by state and output feedback", *transactions on cybernetics*, vol. 45.8, pp. 1587-1596, 2015.
[20] L.iu, Yan-Jun, et al, "Adaptive NN controller design for a class of nonlinear MIMO discrete-time systems", *Transactions on Neural Networks and Learning Systems*, vol. 26.5, pp. 1007-1018,2015.
[21] Yu, Lei, et al, "Design of robust adaptive neural switching controller for robotic manipulators with uncertainty and disturbances", *Journal of Intelligent & Robotic Systems*, vol. 77.3, pp. 571,2015.

8. Appendix

A: Calculation of injected current by Machine

Writing the KVL law between the infinite bus and the output terminal of synchronous generator results:

$$V_t = jX_tI_t + jX_3I_3 + V_B \tag{20}$$

Writing the KCL laws in the middle bus of the power system results:

$$I_3 = I_2 + I_t = \frac{V_2 - V_3}{jX_2} + I_t = \frac{V_2}{jX_2} - \frac{V_3}{jX_2} + I_t \tag{21}$$

By combining the above two equations, we can write:

$$V_t = jX_tI_t + \frac{X_3}{X_2}V_2 - \frac{X_3}{X_2}V_t + \frac{jX_3X_t}{X_2}I_t + jX_3I_t + V_B \tag{22}$$

Each circuit component (voltage and current) in the power system under study can be represented as follows:

$$I_t = I_{td} + jI_{tq}, V_t = V_{td} + jV_{tq} \tag{23}$$

For the internal voltage of the synchronous generator, we have:

$$V_{td} = x_qI_{tq}, V_{tq} = E'_q - X'_dI_{td} \tag{24}$$

By writing all the voltage and current components in the PARK reference frame as well as replacing the dq components related to the terminal voltage and separating the imaginary and real components from each other, we can write:

$$Z_2X_qI_{tq} - Z_3V_{2d} - V_{Bd} = -Z_1I_{tq} \tag{25}$$

$$Z_2E'_q - Z_2X'_dI_{td} - Z_3V_{2q} - V_{Bq} = Z_1I_{td} \tag{26}$$

Note that the infinite bus voltage can be displayed as follows (δ is load angle):

$$V_B = V_{Bd} + jB_{bq} = V_B\sin(\delta) + jV_B\cos(\delta) \tag{27}$$

Therefore, from the above equation, the dq currents injected by the synchronous generator into the network are obtained:

$$I_{tq} = Z_6.M_2.V_{dc}.\cos\delta_2 - Z_7\sin\delta \tag{28}$$

$$I_{td} = Z_{10}E'_q + Z_8.M_2.V_{dc}.\cos\delta_2 + Z_9\cos\delta \tag{29}$$

B: Parameters of power System

Xq=.6; Xd=1; Xdp=0.3; Xt=0.18; Xlb=1; X1=0.18; X2=0.18; X3=0.6; Vdcr=2; Vdci=2; Cdcr=1; Cdci=1; Tdo'=5; M=12; D=0; KA=140; TA=0.015;
Z1 = Xt+(X3*Xt/X2)+X3; Z2=1+(X3/X2); Z3=X3/X2; Z4 = Z2*Xq+Z1; Z5=Z1+Z2*Xpd; Z6=0.5*Z3/Z4; Z7=-abs(VB)/Z4; Z8=-Z3/Z5; Z9 = -abs(VB)/Z5; Z10=Z2/Z5; Z11 = Z6*Vdc*cos(Delta2); Z12=Z6*M2*cos(Delta2) ; Z13 = - (30)

```
6*Vdc*M2*sin(Delta2); Z14 = -Z7*cos(Delta); Z15 = Z8*Vdc*cos(Delta2); Z16 = Z8*M2*cos(Delta2) ; Z17 = -Z8*M2*Vdc*sin(Delta2); Z18 = -Z9*sin(Delta); Z19 = 3/(4*Cdc); Z20 = (Xpd/X2) + (Xt/X2); Z21=1/(2*X2); Z22 = Z21*Vdc*sin(Delta2); Z23 = Z21*M2*sin(Delta2); Z24 = Z21*M2*Vdc*cos(Delta2); Z25= Z20*Z10 + (-1/X2); Z26 = Z22+Z20*Z15; Z27 = Z23+Z20*Z16; Z28 =Z24 + Z20*Z17; Z29= Z20*Z18; Z30=-1/(2*X2); Z31 = (Xq/X2)+(Xt/X2); Z32 = Z30*Vdc*cos(Delta2); Z33= Z30*M2*cos(Delta2); Z34 = -Z30*M2*Vdc*sin(Delta2) ; Z35 = Z32+Z31*Z11; Z36 = Z33+Z31*Z12; Z37 = Z34+Z31*Z13; Z38=Z31*Z14; Z39 = -V1d/ (V1d^2+V1q^2); Z40 = V1q / (V1d^2+V1q^2) ; Z41 = (-Pw*(V1d^2+V1q^2) - (2*V1d) * (-Pw*V1d + Qw*V1q))/ ((V1d^2+V1q^2)^2); Z42 = (Qw*(V1d^2+V1q^2) - (2*V1q) * (-Pw*V1d + Qw*V1q))/ ((V1d^2+V1q^2)^2) ; Z43 = (Z41* 0.5 * Vdc * cos(Delta1)) + (Z42 * 0.5* Vdc * sin(Delta1)) ; Z44 = (Z41*0.5* Vdc * M1* sin(Delta1)) + (Z42*0.5*M1* Vdc * cos(Delta1)) ; Z45 = (Z41*0.5*M1* cos(Delta1)) + (Z42 * 0.5* M1*sin(Delta1)); Z46 = -V1d/(V1d^2+V1q^2); Z47=-V1q/(V1d^2+V1q^2); Temp_48=-(Qw* (V1d^2+V1q^2) - (2*V1d)* (Qw*V1d + Pw*V1q)) / ((V1d^2 + V1q^2)^2) ; Temp_49=-(Pw*(V1d^2+V1q^2) - (2*V1q)*(-Qw*V1d+Pw*V1q)) / ((V1d^2+V1q^2)^2); Z48 = (-.5*Temp_48* M1 * Vdc * sin(Delta1)) + (0.25*Temp_49 * M1* Vdc *cos(Delta1));
Z49 = (0.5*Temp_48* Vdc * cos(Delta1)) + (0.5*Temp_49* Vdc * sin(Delta1)); Z50 = (0.25*Temp_48 * M1* cos(Delta1)) + (0.25 * Temp_49 * M1 * sin(Delta1)); Z51 = Z19 * cos(Delta2) *I2d + Z19 * sin(Delta2)*I2q; Z52 = Z19 * cos(Delta1) *I1d + Z19* sin(Delta1) * I1q; Z53 = -Z19*M1 * sin(Delta1) *I1d + Z19*M1* cos(Delta1)*I1q ; Z54 = -Z19 * M2 * sin(Delta2)* I2d + Z19 * M2 * cos(Delta2) * I2q; Z56 = M2 * Z19 * cos(Delta2); Z57 = M1*Z19* cos(Delta1); Z58 = M2 * Z19 * sin(Delta2) ; Z59 = M1* Z19 * sin(Delta1) ; t_z56 = Z51+Z56*Z26+Z58*Z35; t_z57 = Z52+Z57* Z43+Z59 * Z49; t_z58 = Z53+Z57*Z44+Z59*Z48 ; t_z59 = Z54+Z56*Z28+Z58*Z37; t_z60 = Z52 * Z27+ Z58 * Z36 + Z57*Z45+Z59*Z50; t_z61 = Z25 * Z56; t_z62 = Z29*Z56+Z38*Z58; t_z63 = Z39 * Z57+Z47 * Z59; t_z64 = Z40*Z57+Z46*Z59; a1=Epq + (Xd-Xpd) * Itd; a2 = (Xd-Xpd) * Itq; a3 = Itq; a4=a1 * Z11+a2 * Z15; a5=a1*Z13+a2* Z17; a6=a1 * Z14+a2 * Z18; a7=a1 * Z12 + a2 * Z16; a8=a3+a2*Z10; a9=Vtd * Xq/abs(Vt); a10=Vtq/abs(Vt); a11=- Xpd*Vtq/abs(Vt); a12 = a9*Z11+a11*Z15; a13= a9*Z12+a11*Z16; a14 = a10+a11*Z10; a15=a9*Z13+a11*Z17; a16=a9*Z14+a11*Z18; s = -(Xd-Xpd);
```